Clinical and Translational Radiation Oncology 41 (2023) 100630

Contents lists available at ScienceDirect

Clinical and Translational Radiation Oncology

journal homepage: www.sciencedirect.com/journal/clinical-and-translational-radiation-oncology

Impaired DNA double-strand break repair and effective radiosensitization of HPV-negative HNSCC cell lines through combined inhibition of PARP and Wee1

Agnes Oetting [a,b], Sabrina Christiansen [a,b], Fruzsina Gatzemeier [a,b], Sabrina Köcher [a,b], Lara Bußmann [b,c], Arne Böttcher [b], Katharina Stölzel [b], Anna Sophie Hoffmann [b], Nina Struve [a,c], Malte Kriegs [a], Cordula Petersen [a], Christian Betz [b], Kai Rothkamm [a], Henrike Barbara Zech [a,b,c,1], Thorsten Rieckmann [a,b,1,*]

[a] Department of Radiotherapy, University Medical Center Hamburg Eppendorf, Germany
[b] Department of Otorhinolaryngology, University Medical Center Hamburg Eppendorf, Germany
[c] Mildred-Scheel Cancer Career Center HaTriCS4, University Medical Center Hamburg-Eppendorf, Germany

ARTICLE INFO

Keywords:
Head and neck cancer
Radiotherapy
Radiosensitization
PARP
Wee1
DNA repair
Cell-cycle checkpoint

ABSTRACT

Objectives: In head and neck squamous cell carcinoma (HNSCC), tumors negative for Human Papillomavirus (HPV) remain a difficult to treat entity and the morbidity of current multimodal treatment is high. Radiotherapy in combination with molecular targeting could represent suitable, less toxic treatment options especially for cisplatin ineligible patients. Therefore, we tested dual targeting of PARP and the intra-S/G2 checkpoint through Wee1 inhibition for its radiosensitizing capacity in radioresistant HPV-negative HNSCC cells.

Materials and methods: Three radioresistant HPV-negative cell lines (HSC4, SAS, UT-SCC-60a) were treated with olaparib, adavosertib and ionizing irradiation. The impact on cell cycle, G2 arrest and replication stress was assessed through flow cytometry after DAPI, phospho-histone H3 and γH2AX staining. Long term cell survival after treatment was determined through colony formation assay and DNA double-strand break (DSB) levels were assessed through quantification of nuclear 53BP1 foci in cell lines and patient-derived HPV± tumor slice cultures.

Results: Wee1 and dual targeting induced replication stress but failed to effectively inhibit radiation-induced G2 cell cycle arrest. Single as well as combined inhibition increased radiation sensitivity and residual DSB levels, with the largest effects induced through dual targeting. Dual targeting also enhanced residual DSB levels in patient-derived slice cultures from HPV-negative but not HPV+ HNSCC (5/7 vs. 1/6).

Conclusion: We conclude that the combined inhibition of PARP and Wee1 results in enhanced residual DNA damage levels after irradiation and effectively sensitizes radioresistant HPV-negative HNSCC cells. *Ex vivo* tumor slice cultures may predict the response of individual patients with HPV-negative HNSCC to this dual targeting approach.

1. Introduction

Standard treatment of locally advanced head and neck squamous cell carcinoma (HNSCC) consists of either primary cisplatin-based chemoradiation or primary surgery followed by adjuvant (chemo)radiation. Treatment related morbidity is high due to early and late, partly irreversible, side effects, such as high grade mucositis, dysphagia, xerostomia, hearing loss or nephrotoxicity. For patients with human Papillomavirus-negative (HPV-) HNSCC cure rates are still unsatisfactory due to frequent radio- and chemoresistance [1–3]. Molecular targeting with the aim of tumor radiosensitization may present an alternative to concomitant chemotherapy. The anti-EGFR antibody cetuximab is approved in the curative setting but considerable doubts exist regarding its efficacy when combined with (chemo)radiation [4].

* Corresponding author at: University Medical Center Hamburg-Eppendorf, Martinistrasse 52, 20246 Hamburg, Germany.
E-mail address: t.rieckmann@uke.de (T. Rieckmann).
[1] Equal contribution.

https://doi.org/10.1016/j.ctro.2023.100630
Received 12 December 2022; Received in revised form 13 April 2023; Accepted 17 April 2023
Available online 20 April 2023

Apart from targeting signal transduction pathways, direct inhibition of the DNA damage response and DNA double-strand break (DSB) repair are the most intensively studied approaches. A potential way to increase efficacy is the combined inhibition of two targets in order to either achieve a more complete pathway inhibition, block a potentially compensating pathway or target two distinct pathways to achieve synthetic lethality or synergistic radiosensitization [5,6]. The combined inhibition of PARP (Poly(ADP-ribose) polymerase) and the intra-S/G2 cell cycle checkpoints through targeting of the ATR/Chk1/Wee1 axis is a strategy that has proven to be effective in preclinical models of pancreatic, and non-small cell lung cancer as well as glioblastoma [7–11]. Poly(ADP-ribose) polymerization (PARylation) by PARP1/2 is an early event in single strand break repair and, through the backup repair pathway alternative end-joining (alt-EJ), in part also in DSB repair. In both cases PAR chains mark the lesion and recruit downstream DNA repair factors [12,13]. Interfering with single-strand break repair through PARP inhibition leads to enhanced collisions of single-strand lesions and replication forks during S phase and a functional homologous recombination (HR) machinery is required to resolve these structures. As alt-EJ requires DNA end resection, which occurs mainly in S- and G2-phase, its inhibition through PARP targeting will also mainly affect S as well as G2 phase cells. Importantly, PARP inhibition also traps PARP on the DNA, which generates an obstacle for replication and repair. Sole PARP inhibition is especially effective in tumors with HR deficiencies and is, amongst other settings, approved in breast, ovarian, prostate and pancreatic cancer with BRCA mutations [14]. With regard to the combination with radiation, PARP inhibition is a well-established approach for tumor radiosensitization but at present not approved in any tumor entity [15].

Cell cycle checkpoints represent another important player in the DNA damage response. They provide additional time for DNA repair before the cells have to enter the replicative S phase or pass through mitosis with the risk of mitotic cell death when still harboring unrepaired DSBs. As the vast majority of HNSCC is deficient for p53 and, as a consequence, also for G1 cell cycle arrest, irradiated HNSCC cells mostly rely on the G2/M checkpoint to halt the cell cycle before passing through mitosis [16]. Targeting components of the ATR/Chk1/Wee1 axis can interfere with intra-S and G2 arrest, causes replication stress and was further reported to impair DSB repair through HR and all these effects have the potential to radiosensitize the affected cells [17]. With regard to the combination with (chemo)radiation in HNSCC, initial studies have been conducted for both, PARP and cell cycle checkpoint inhibitors. It has to be noted, that when combined with radiotherapy in HNSCC, both classes of agents and especially PARP inhibitors, require a profound dose reduction as compared to what can be applied in monotherapy. So apparently, tolerability is an issue, especially when the inhibitors are added to chemoradiation [18–21]. Therefore, testing these approaches as an alternative to chemoradiation, e.g. for cisplatin-unfit patients, may be a more promising approach and attempts to further escalate current standard regimes should be considered with caution.

We had recently demonstrated effective radiosensitization of HPV+ HNSCC cell lines through enhanced DNA damage caused by PARP inhibition in the S and G2 phase plus subsequent inhibition of the otherwise long lasting radiation-induced G2 arrest by Wee1 inhibition forcing the cells to pass mitosis with unrepaired DNA DSBs [22]. Here, we assessed the potential of combined PARP and Wee1 inhibition through olaparib (AZD-2281) and adavosertib (AZD-1775) to radiosensitize radioresistant HPV- HNSCC cell lines.

2. Material and methods

2.1. Cells and cell culture

All cell lines were grown in RPMI (Sigma-Aldrich) supplemented with 10% fetal bovine serum (FBS) (Biochrom AG), 1% Penicillin/Streptomycin (Sigma) at 37° C, 5% CO_2 and 100% humidification. HPV-HNSCC cells HSC4, SAS and UT-SCC-60A were described previously [23]. Tumor cell line identity was validated by a short tandem repeat multiplex assay (Applied Biosystems). PARP inhibition was performed using 1 μM olaparib (MyBiosource), Wee1 inhibition was performed using 240 nM adavosertib (Selleckchem).

2.2. Cell proliferation

For cell proliferation analysis, cells were seeded into T25 cell culture flasks and after 4 h treated with inhibitors. The numbers of resulting cells were assessed after 5 days using a Coulter counter (Beckmann-Coulter).

2.3. Cell cycle assessment

Cells were harvested, fixed with 70% ethanol, briefly washed with PBS/0.5% BSA/0.1% Triton X-100 and subsequently incubated with PBS/1% BSA/0.2% Triton X-100/DAPI (4′,6-Diamidin-2-phenylindol, 1 μg/ml) for 30 min at room temperature in the dark. Cells were washed once with PBS/0.5% BSA/0.1% Triton X-100 before flow cytometric analysis using a MACSQuant10 with MACSQuantify Software (Miltenyi Biotec). The proportion of cells in the respective cell cycle phases was calculated using ModFit LT^{TM} software (Verity Software House, Inc.).

2.4. X-irradiation

Cells were irradiated at room temperature with 200 kV X-rays (Gulmay RS225, Gulmay Medical Ltd.; 200 kV, 15 mA, 0.8 mm Be + 0.5 mm Cu filtering; dose rate of 1.2 Gy/min).

2.5. Flow cytometric protein quantification

Flow cytrometric measurement of relative protein staining intensity in relation to the cell cycle phase was performed on a MACSQuant10 with MACSQuantify and Flowlogic Software (Miltenyi Biotec & Inivai) using DAPI as nuclear counter stain. In brief, cells were harvested, fixed with PBS/4% formaldehyde for 10 min and then permeabilized and blocked with PBS/1% BSA/0.2% Triton X-100 for a minimum of 30 min at room temperature or overnight at 4 °C. The cells were subsequently incubated (1 h; room temperature) with the primary antibody (rabbit anti-P-Histone3 (#06-570, Millipore); mouse-anti-γH2AX (clone JBW301, Millipore)) in blocking solution, washed three times with PBS/0.5% BSA/0.1% Triton X-100 before incubation (1 h; room temperature) with the second antibody + DAPI in blocking solution and were then washed again three times.

2.6. Colony formation assay

Radiosensitization was determined using delayed plating colony formation assay. Exponentially growing cells were treated with inhibitor and irradiated after 2 h. Twenty-four hours post irradiation the cells were seeded in defined low numbers into 6-well cell culture wells (triplicates per condition) without addition of inhibitors. Incubation time until colony formation varied between cell lines from 10 to 14 days; irradiated samples were allowed to grow for an extended period of time, as colony formation was apparently delayed. The number of colonies containing more than 50 cells was assessed.

2.7. Patient sample collection

Fresh tumor tissue was obtained from OPSCC patients treated at the University Medical Center Hamburg-Eppendorf. HPV and p16 status of the tumors were assessed during routine clinical characterization by E6 and E7 PCR (MY09/11 primer set) and subsequent sequencing of PCR products and by immunohistochemical staining for p16 (anti-p16

antibody; DCS-50.1/A7; Nordic-MUbio) respectively. Samples were collected during surgery using a gentle non-traction method of sharp cutting and were immediately transferred into sterile DMEM medium for transportation. Tissue preparation was initiated within 30 min from collection. Sample collection and processing was performed in accordance with the World Medical Association Declaration of Helsinki and the guidelines for experimentation with humans by the Chambers of Physicians of the State of Hamburg. All patients gave written informed consent for their excised tissue to be used for research purposes. Collection of head and neck tumor tissue in the context of the ENT biobank was notified to the Hamburg Commissioner for Data Protection and Freedom of Information (HmbBfDI) in accordance with local laws (§12 HmbKHG) and the local ethics committee (Ethics commission Hamburg WF-049/09, WF- PV5119). Clinical data analysis was approved via patient consent and by local laws (§7, §8, §12 HmbKHG).

2.8. Ex vivo tumor slice culture

Cultivation of tumor slices was performed as described previously [24]. Fresh tumor samples were initially divided by a scalpel and then cut into 400 μm slices using a tissue chopper (McIllvine) or, in case the texture did not allow precise machine cutting, using a scalpel. Tissue slices were placed on Millicell® cell culture inserts (0.4 μm, 30 mm diameter, Merck) in 6-well dishes containing 1 ml Dulbecco's modified Eagle medium (DMEM) (Gibco-Invitrogen) supplemented with 10% heat inactivated (65 °C; 30 min) fetal bovine serum (FBS) (Biochrome), 1% Penicillin/Streptomycin and 1% Amphotericin B (both Gibco). Slice cultures were incubated at the air–liquid-interface at 37 °C, 5% CO2 and 100% humidification over night for recovery and re-oxygenation. Medium was exchanged after one day and slice cultures were supplemented with DMSO or inhibitors and irradiated with 0 or 3 Gy and incubated for 24 h before fixation using PBS/4% formaldehyde for 1 h.

2.9. Immunofluorescence

Cells grown on glass cover slips were fixed with PBS/4% formaldehyde for 10 min and permeabilized/blocked for a minimum of 30 min at room temperature or overnight at 4 °C in PBS/1% BSA/0.2 %Triton X-100. The cells were subsequently incubated for 1 h at room temperature with the primary antibodies (rabbit anti-53BP1 (NB100-305, Novus Biologicals); mouse anti-γH2AX (clone JBW301, Merck)) in blocking solution, washed four times with PBS/0.5% BSA/0.1% Triton X-100 before incubation with the secondary antibodies plus DAPI (1 h; room temperature) and were then washed again four times.

For tumor slice cultures, fixed samples were washed twice with PBS/20% sucrose for 1 h. Samples were frozen and stored at −80 °C in TissueTek (Serva) until cryoslices (5 μm) were prepared using a CryoStar NX70 Microtome (Thermo Scientific). Cryoslices were short-term stored at −20 °C. For immunofluorescent staining, cryoslices were subsequently incubated in aceton and PBS for 10 min each and afterwards in PBS/1% SDS for 1 h before blocking in PBS/3% BSA over night at 4 °C. The slices were subsequently incubated for 1 h at room temperature with the primary antibodies (rabbit anti-53BP1 (NB100-305, Novus Biologicals); mouse anti-p63 (clone 4A4, Abcam)) in blocking solution, washed three times with PBS/0.5% Tween20 before incubation with the secondary antibodies plus DAPI (1 h; room temperature) and were then washed again three times.

Stained cells and slice cultures were mounted in Vectashield mounting medium (Vector Laboratories) and inspected using an AxioObserver.Z1 fluorescence microscope with Apotome and Axiovision Software (Zeiss). 53BP1 foci per nucleus were manually counted using stack images in maximum intensity projection. Nuclei with ≥ 20 foci were scored as 20.

In the case of slice cultures only nuclei positive for the SCC marker p63 were assessed and since nuclei in cryosections are randomly cut, the whole area of p63 co-stained nuclei was quantified through DAPI-based image masks using ImageJ to generate a value of foci/nuclear area. These values are finally presented as foci per nucleus after normalization to the average area of unruffled tumor nuclei as determined from multiple OPSCC specimens as previously described [24].

2.10. Data evaluation

Data analysis was performed using Excel (Microsoft) and GraphPad Prism 6 (GraphPad Software). All experiments were performed at least three times, unless stated otherwise. Values presented are mean ± SD unless indicated otherwise. Single experiments always contained the full set of substances and radiation doses as indicated.

3. Results

Before combining PARP and Wee1 inhibition with radiation in HPV-HNSCC cell lines, we first assessed the influence of dual inhibition on cell proliferation, to estimate potentially relevant synergistic effects. PARP inhibition through 1 μM olaparib very moderately reduced the resulting cell counts after 5 days of incubation, whereas Wee1 inhibition through 240 nM adavosertib resulted in a profound and significant reduction in all strains. Dual inhibition demonstrated the overall biggest growth inhibition but the differences between dual and sole Wee1 inhibition did not reach significance **(**Fig. 1**)**. Numerically, the cell numbers after dual inhibition in HSC4 and UT-SCC-60a reached only 74.3% and 64.5% of the numbers calculated for a strictly additive growth inhibition and we cannot rule out that some synergy may exist. But as these data do not provide a clear hint for a general and prominent effect in HNSCC cells, in line with a recent report [25], this was not investigated in detail.

3.1. Cell cycle arrest and replication stress

Irrespective of their HPV-status HNSCC cells are mostly not capable of arresting in the G1 phase after DNA damage induction through ionizing irradiation due to functional p53 deficiency. This increases the dependency on the radiation-induced G2 arrest to avoid the potentially lethal passage through mitosis and nuclear division with unrepaired DSBs, which provides a rationale for G2 arrest inhibition through Wee1 targeting. HPV- HNSCC cells mostly demonstrate a briefer and less pronounced G2 arrest compared to the more radiosensitive HPV+ HNSCC cells [26,27] but in the first couple of hours HPV- cells may also depend on halting the cell cycle to provide more time for DSB repair. Therefore we tested the fraction of cells reaching mitosis at 5 h and the cell cycle distribution at 12 and 24 h after irradiation. At 5 h the fraction of cells positive for the mitotic marker phospho-histone H3 was severely diminished after irradiation as well as after irradiation plus PARP-inhibition indicating effective G2 arrest **(**Fig. 2**A,B)**.

Wee1 inhibition moderately to slightly impaired the arrest in these HPV- HNSCC strains, and in HSC4 and SAS cells, this limited capacity was further reduced when combined with PARP inhibition.

At a later time point of 12 h after irradiation **(**Fig. 2**C, top)** solvent treated cells demonstrated different degrees of radiation-induced G2 arrest. At 24 h after irradiation **(**Fig. 2**C, bottom)**, which is the peak time point for G2 arrest in HPV+ HNSCC cells [40], we observed a normalisation of the cell cycle distribution in HSC4 and UT60a indicative of effective DSB repair. A still profound G2 arrest was only observed in SAS cells after the higher radiation dose of 6 Gy. PARP inhibition in part resulted in a moderately increased amount of cells in the G2 phase at both time points in line with some capacity to induce higher levels of DNA damage. In contrast, Wee1 inhibition resulted in somewhat reduced numbers of cells in the G2 phase in HSC4 and UT60a cells at 12 h after irradiation indicating some limited ability to interfere with radiation-induced G2 arrest. A similar, moderate effect was observed when comparing combined Wee1/PARP inhibition to sole PARP-Inhibition. Unexpectedly, at the later time point of 24 h after

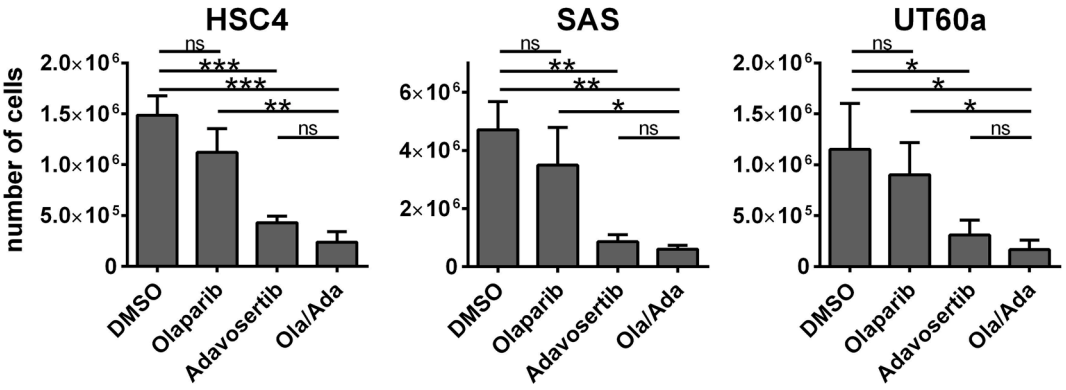

Fig. 1. Effect of PARP and Wee1 inhibition on cell proliferation. 12,500 cells were seeded and after 4 h treated with inhibitors as indicated. Five days later the respective numbers of cells were assessed. Significant changes are indicated with *, ** and *** indicating $p < 0.05$, $p < 0.01$ and $p < 0.001$, respectively (two-tailed Student's *t*-test). ns: not significant. Results are based on 3 individual experiments per cell line.

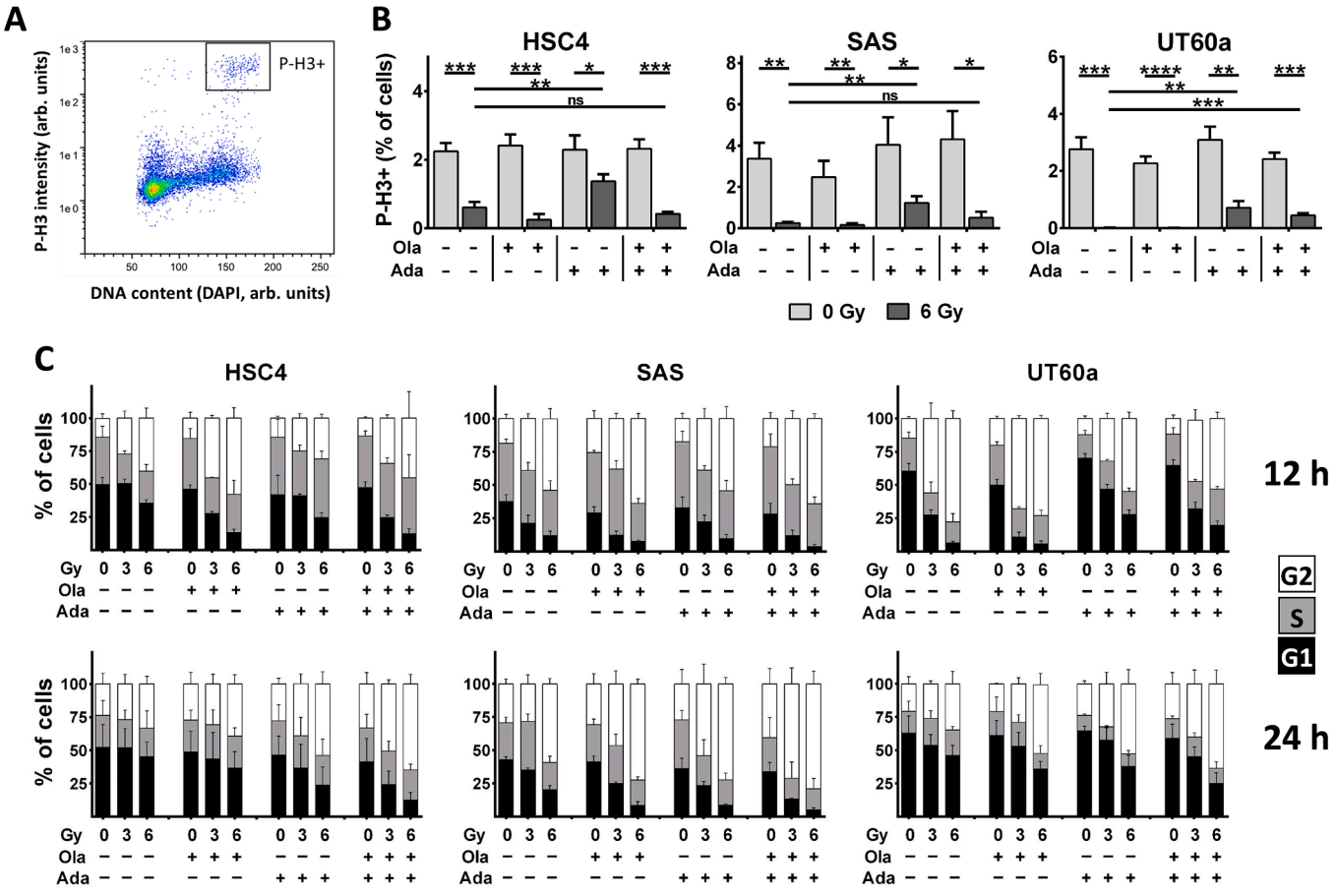

Fig. 2. Radiation-induced G2 arrest. (A,B) Fraction of mitotic cells. Exponentially growing cells were treated for 2 h with the inhibitors as indicated before irradiation with 0 or 6 Gy. Five hours after irradiation cells were fixed and stained for phospho-histone H3 to assess the number of mitotic cells. Significant changes are indicated with *, **, *** and **** indicating $p < 0.05$, $p < 0.01$, $p < 0.001$ and 0.0001, respectively (two-tailed Student's *t*-test). ns: not significant. Results are based on 3 individual experiments per cell line. (**A**) Gating of phospho-histone H3 positive cells. (**B**) Quantification of the mitotic fraction. P–H3: Phospho-Histone H3 (**C**) Cell cycle distribution at 12 and 24 h after irradiation. Cells were treated and irradiated as in A and B. At 12 and 24 h after irradiation the cells were fixed and the cell cycle distribution assessed by DAPI staining and flow cytometry. Results are based on 3 individual experiments per cell line.

irradiation, we observed an even enhanced number of G2 phase cells after sole and combined Wee1 inhibition as compared to the respective solvent controls. These results are in contrast to our previous observations in HPV+ HNSCC cells, where sole and combined Wee1 inhibition enhanced recovery of the cell cycle distribution [22]. The prolonged cell cycle disturbances observed here confirm the inability of sole and combined Wee1 inhibition to effectively inhibit the radiation-induced G2 arrest in HPV- HNSCC cells as observed after 5 h (Fig. 2**B**). Furthermore, the even increased fractions of G2 phase cells may suggest enhanced DNA damage levels at 24 h after irradiation that are still capable of triggering the cell cycle checkpoint response.

Unrestrained CDK2 activity as a result of Wee1 inhibition was reported to cause severe replication stress due to unscheduled firing of dormant origins, resulting in too many active replication forks and

nucleotide depletion [28,29]. Enhanced replication stress after Wee1 and also combined PARP/Wee1 inhibition was previously described for hepatocellular carcinoma, NSCLC and HPV+ HNSCC cells [10,22,30]. Upon subsequent fork stalling, or separation of the helicases and the polymerase complexes, stretches of single-strand DNA (ssDNA) are generated and recognized through the ATR kinase, leading to the decoration of such areas by the DNA damage and replication stress marker γH2AX. Indeed, sole inhibition of Wee1 resulted in a clear increase in γH2AX intensity in S- and partly G2 phase cells but not G1 phase cells in all HPV- HNSCC strains. In HSC4 but not SAS or UT-SCC-60a cells, sole PARP inhibition also increased γH2AX intensity in S/G2 phase cells but to a lesser extent that did not reach significance in our experiments ($p = 0.063$). Combined inhibition did not increase γH2AX intensity or the fraction of cells with enhanced γH2AX intensity as compared to sole Wee1 inhibition (Fig. 3**A,B** Supplementary Fig. 1). Additional irradiation further increased γH2AX signal intensity in G1 and S/G2-phase cells but the impact varied between cell lines and treatments. In G1-phase cells, especially dual inhibition and the higher dose of 6 Gy induced a considerable increase in γH2AX signal intensity. For S/G2-phase cells, when considering also the cell cycle changes after sole or combined adavosertib treatment + irradiation **(see** Fig. 2**C bottom)**, it becomes apparent that in all strains a large fraction of cells becomes arrested for prolonged times in S/G2 phase under stressed conditions.

3.2. DSB repair, cell survival and prediction

For the quantification of residual DSBs after irradiation, we performed co-staining of the DSB surrogate markers γH2AX and 53BP1. As expected from the flow cytometric assessment, Wee1 inhibition resulted in a considerable amount of cells demonstrating pan-nuclear γH2AX staining in fluorescence microscopy with and without irradiation with 2

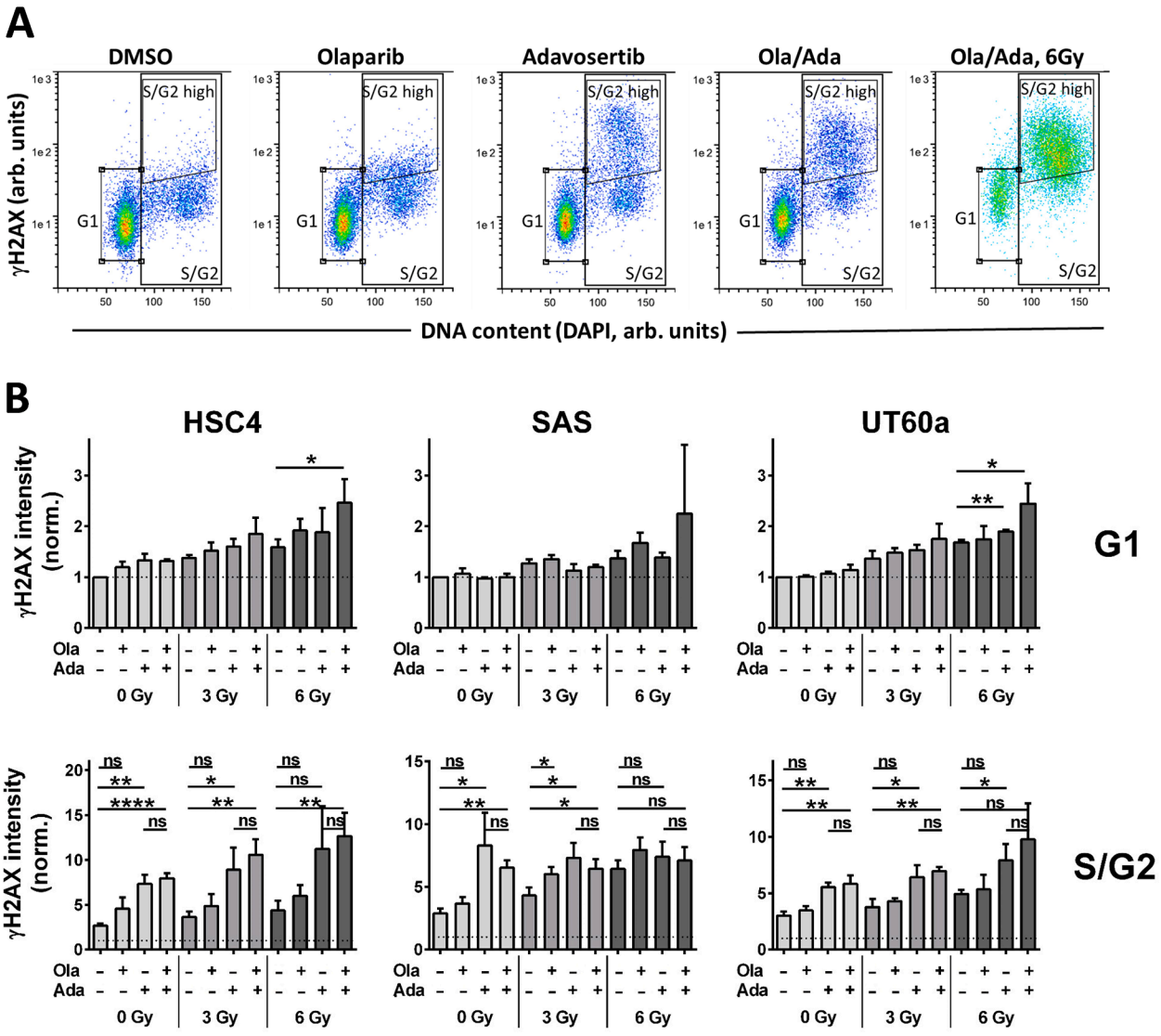

Fig. 3. Effect of PARP and Wee1 inhibition on γH2AX staining intensity. Cells were treated with inhibitors as indicated for 2 h before irradiation and were then fixed 24 h later followed by staining and flow cytometric assessment of γH2AX intensity. (A) Examples of the flow cytometric measurement of HSC4 cells and depiction of the gating strategy for cells in the G1 phase, in S/G2 and cells in S/G2 demonstrating enhanced γH2AX levels ("S/G2 high", see Suppl. Fig. 1). (B) Relative staining intensity of G1 and S/G2 phase cells. Bars depict the mean of the median values of the individual experiments. Staining intensity was normalized to the values of the non-irradiated, DMSO treated G1 phase cells of each experiment, also indicated by the dotted lines. G1 phase cells only demonstrated few significant differences, which are all indicated within the individual irradiation dose groups (except for 0 Gy/DMSO based combinations because of normalized values). Significant changes are indicated with *, **, *** and **** indicating $p < 0.05$, $p < 0.01$, $p < 0.001$ and 0.0001, respectively (two-tailed Student's t-test). ns: not significant. Results are based on 3 individual experiments per cell line.

Gy (Fig. 4**A,B**). Quantification of residual DSBs was therefore performed using 53BP1, which is far less responsive towards replication stress. While we had previously not observed a general increase in radiation-induced 53BP1 foci at 24 h after 2 Gy irradiation upon combined PARP/Wee1 inhibition in HPV+ HNSCC cells [22], we observed clearly and significantly enhanced foci levels in all three HPV- strains as compared to DMSO treatment (Fig. 4**C,** Supplementary Fig. 2**A**). Regarding single inhibition, we observed a stronger increase after Wee1 as compared to PARP inhibition in HSC4 and UT-SCC-60a and a stronger effect of PARP than Wee1 inhibition in SAS cells, with effects partly not reaching significance. Dual inhibition most effectively increased the fraction of heavily damaged cells with at least 20 foci per nucleus at 24 h after 2 Gy irradiation, in line with the highest fraction of cells arrested in the G2 phase at this time point after a comparable dose of 3 Gy (Fig. 2**C**, Fig. 4**D**). Importantly, the fraction of cells with especially low numbers of residual radiation-induced DSBs, which are the ones most likely to survive treatment, was decreased upon all treatments and to the largest extent upon dual inhibition (Fig. 4**E,** Supplementary Fig. 2**B**). Excluding cells with pan-nuclear γH2AX signals from the analyses yielded highly similar results (Supplementary Fig. 2**C-E**), suggesting that severe replication stress in a subfraction of S phase cells is not an essential contributor to the observed effects.

In line with the most severe increase in residual DSBs, we also observed the most profound radiosensitization upon combined treatment in delayed plating colony formation assays (Fig. 5**A**). Single inhibition also induced radiosensitization but to a varying and overall lesser extent. Cell survival after irradiation ± molecular targeting was significantly associated with residual DSBs, as well as with the fractions of cells showing especially high and low DSB numbers after irradiation (Supplementary Fig. 3**A**). The survival of cells under sole Wee1 or combined inhibition without irradiation was far less affected in the colony formation assays with overall 26 h of inhibitor treatment as compared to the profound effects on proliferation depicted in Fig. 1. This indicates a cytostatic rather than a cytotoxic effect at the used concentration of 240 nM adavosertib (Supplementary Fig. 3**B**).

To test whether residual DSB repair foci could potentially serve as a predictive marker for the response towards combined PARP/Wee1 inhibition, we further assessed residual DSB repair foci levels after irradiation in *ex vivo* cultivated tumor slice cultures derived from patients with HPV- and also HPV+ disease (Supplementary Table 1). Without inhibition, HPV+ tumors – compared to HPV- ones – demonstrated more variable and on average enhanced residual 53BP1 foci numbers at 24 h after irradiation. In line with the previously described cell line data of HPV+ HNSCC [22], only 1 in 6 HPV+ tumor slice cultures demonstrated a moderately enhanced foci number when PARP/Wee1 inhibitors were added prior to irradiation, while in HPV- slice cultures 5 in 7 samples demonstrated a mostly clear (Fig. 5**B, left**) and on average significant (Fig. 5**B, right**) increase, corresponding well to the also clearly increased foci level in the three radioresistant HNSCC cell lines (**see** Fig. 4**C**).

4. Discussion

Locally advanced HPV- HNSCC have remained a tough to treat tumor entity with currently still unsatisfactory cure rates and an exceptionally high treatment related morbidity from current multimodal regimes. The anti-EGFR antibody cetuximab was believed to be a less toxic and effective alternative to concurrent cisplatin-based chemotherapy but various recent studies in HPV+ and HPV- HNSCC have raised serious concerns regarding both its efficacy and toxicity when combined with

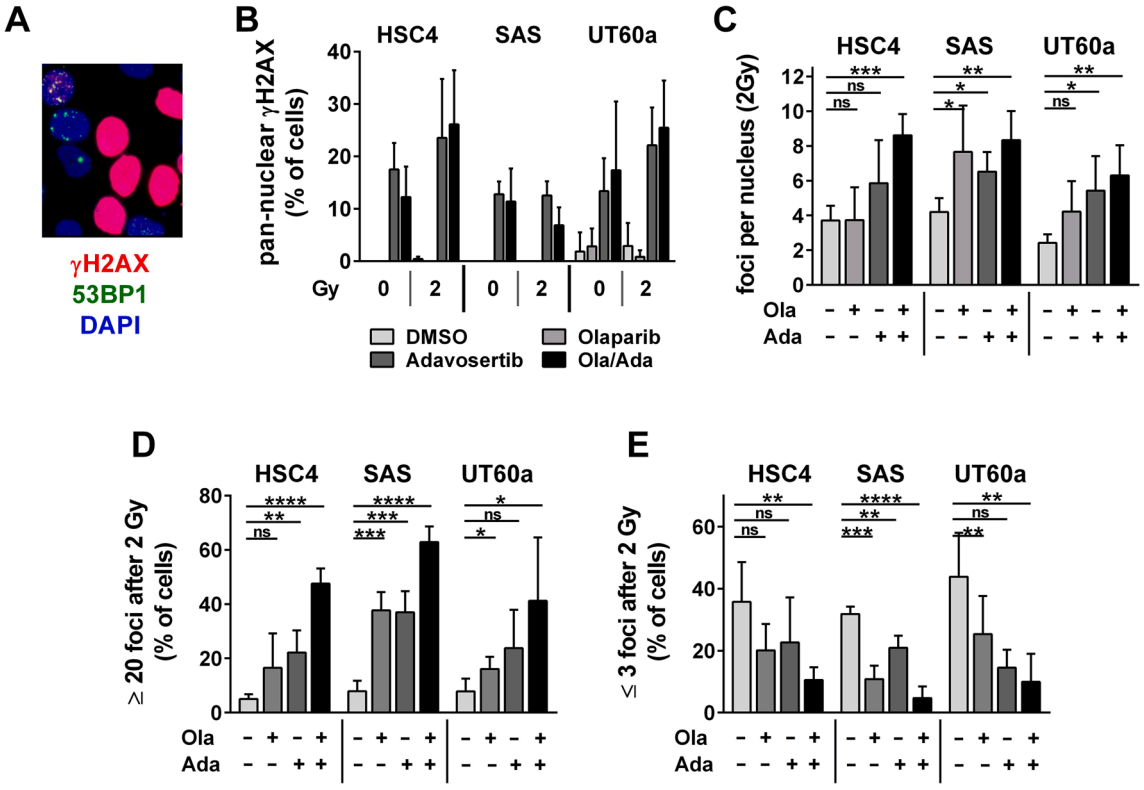

Fig. 4. Effect of PARP and Wee1 targeting on DSB repair. Cells were treated with inhibitors and after 2 h irradiated with 2 Gy as indicated. After 24 h cells were fixed, stained for γH2AX, 53BP1 and DAPI and the level of residual DSB repair foci was assessed through fluorescence microscopy. **(A)** Example of immunofluorescence co-staining. **(B)** Quantification of cells with pan-nuclear γH2AX staining. **(C)** Mean number of radiation-induced nuclear 53BP1 foci after 2 Gy (0 Gy values subtracted). **(D)** Fraction of cells with ≥ 20 53BP1 nuclear foci after 2 Gy. **(E)** Fraction of cells with especially low numbers of 53BP1 nuclear foci after 2 Gy using a threshold of ≤ 3. Significant changes are indicated with *, **, *** and **** indicating $p < 0.05$, $p < 0.01$, $p < 0.001$ and 0.0001, respectively (two-tailed Student's *t*-test). ns: not significant. Results are based on 4 individual experiments per cell line.

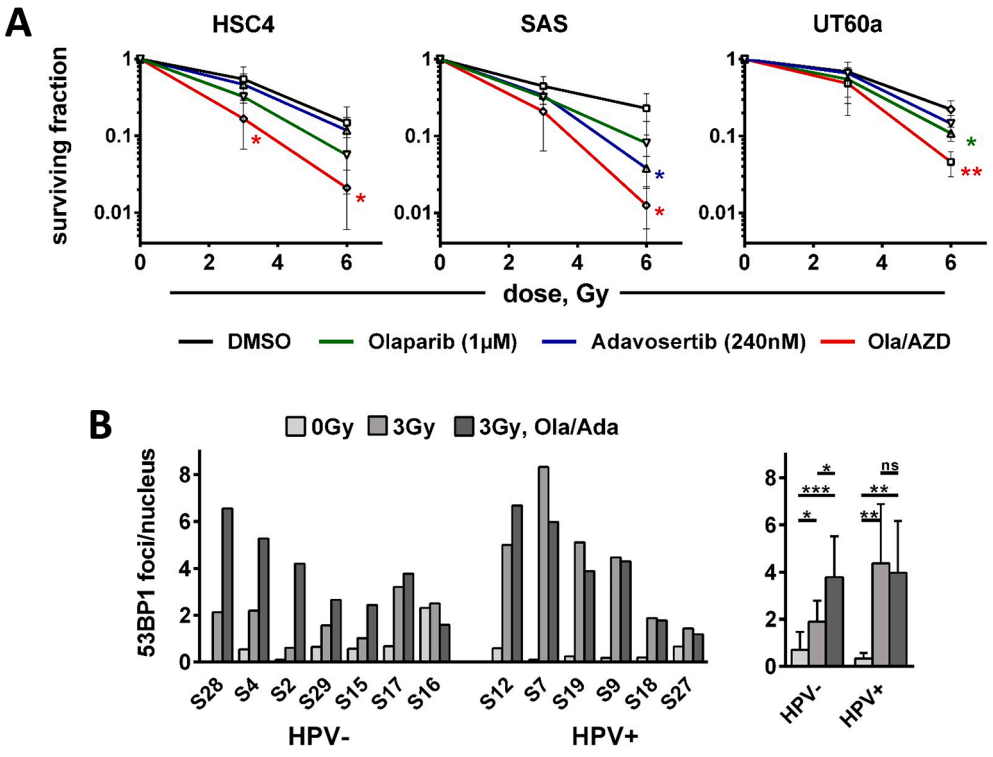

Fig. 5. Radiosensitization in colony formation assays and DSB repair analysis in patient-derived tumor slice cultures. (A) Radiosensitization. Exponentially growing cells were seeded and on the next day treated with inhibitors and irradiated 2 h thereafter as indicated; 24 h later, irradiated cells were seeded in low, defined numbers for colony formation. Significance was assessed for solvent control vs. targeting. In case of a statistically significant difference the respective dose points were marked with asterisks with * and **, indicating $p \leq 0.05$ and $p \leq 0.01$, respectively (two-tailed Student's t-test). Results are based on 4 individual experiments per cell line. (B) Patient-derived tumor slice cultures. After 24 h of ex vivo culture, tumor slices were treated with or without inhibitors for 2 h before irradiation as indicated. After another 24 h, cultures were fixed and processed for 53BP1 staining. Bars represent the mean 53BP1 foci numbers per DAPI area normalized to the average DAPI area of unruffled tumor nuclei. 0 and 3 Gy values were in part presented previously [24]. Left: Single measurements of individual samples. Right: Average values per group. Significant changes are indicated with *, ** and ***, indicating $p \leq 0.05$, $p \leq 0.01$ and $p \leq 0.001$, respectively (two-tailed Student's t-test). ns: not significant.

radiation [4,31]. Large efforts are currently being made to advance immune checkpoint inhibition (ICI) into the curative setting in HNSCC but also here the presently available results of phase III studies of concurrent treatment with ICI and (chemo)radiation have failed to prove efficacy [32–34]. Overall, novel approaches for the curative treatment of HPV- HNSCC are still required and a concurrently applied radiosensitizer may still enable neoadjuvant or subsequent ICI, where it may be more potent. In this regard the dual targeting approach described here may represent a possible option, especially as an alternative for patients unfit for cisplatin-based concurrent chemotherapy.

Ex vivo testing of the patients' biopsy material for enhanced radiation-induced residual DSBs could potentially enable personalized prediction of efficacy with results obtainable within 3 days after biopsy. In previous work using DSB repair foci analyses in *ex vivo* slice cultures, the DSB repair capacity of *ex vivo* irradiated experimental HNSCC xenograft samples correlated well with the results after *in vivo* irradiation [35]. Furthermore, DSB repair in patient-derived *ex vivo* slice cultures from different tumor entities resembled their clinical radiation sensitivity and DSB repair capacity in HPV+ OPSCC slice cultures was associated with pack years of smoking [24,36]. With regard to molecular targeting, the presence or lack of an increase in residual DSB levels in prostate cancer cell lines matched well between the established *in vitro* setting and slice cultures derived from xenograft tumors after PARP inhibition and after antiandrogen therapy [37,38]. Furthermore, we had recently observed a differential effect of ATM inhibition on residual DSB repair foci in HPV- and HPV+ patient-derived HNSCC slice cultures, which also corresponded well to the effects observed in HPV- and HPV+ HNSCC cell lines [24,39]. Together, these data clearly speak in favor of the robustness of the *ex vivo* approach and warrant further research into its utilization for predicting individual tumor responsiveness towards radiation and towards specific radiosensitization approaches.

Mechanistically, radiosensitization through combined PARP and S/G2 checkpoint inhibition in previous work was mostly attributed to DNA repair defects through PARP inhibition including PARP trapping and induction of replication stress plus inhibition of subsequent G2 arrest through ATR/Chk1 or Wee1 inhibition [8–10]. Regarding the latter, our results in radiosensitive HPV+ HNSCC cells did not point towards a prominent role of replication stress under combined PARP and Wee1 inhibition plus irradiation. Instead, it highlighted a role for the inhibition of the – in these cells especially profound – G2 arrest, since we did not observe overall increased residual DSB repair foci but instead a transition of DSB-carrying cells from the G2 to the G1 cell cycle phase and a normalization of the cell cycle distribution at 24 h after irradiation [22]. In contrast, in all three radioresistant HPV- HNSCC strains used here, dual inhibition had only very moderate effects on G2 arrest at 5 and 12 h after irradiation while at 24 h dual as well as sole Wee1 inhibition even resulted in a clear increase of G2 and a corresponding decrease of G1 phase cells. These cell cycle disturbances were accompanied and presumably caused by an increase in non-repaired DSBs at that time point. This phenotype indicates a prominent role of enhanced DNA damage for the observed radiosensitization, likely due to impaired DSB repair processes. So while both, HPV+ and HPV- HNSCC cells were effectively radiosensitized through the dual targeting approach, the mechanisms differ, which was also reflected in the comparison of patient-derived tumor slice cultures, where residual DSBs were only slightly increased in 1/6 HPV-positive patient-derived OPSCC specimens but profoundly in 4/7 HPV-negative ones. Overall, our preclinical data presented here suggest that combined PARP/Wee1 inhibition could represent an effective approach for the radiosensitization of HPV-negative HNSCC and an estimation of the susceptibility of individual tumors through predictive *ex vivo* testing may be more suitable for HPV- than HPV+ tumors.

Funding

This work was supported by the German Cancer Aid (Deutsche Krebshilfe, grant 70113259; KR, SK, TR) and the German Federal Minstry of Education and Research (BMBF, grant 02NUK032; KR, MK, TR).

Role of the Funding Source

The funding sources had no influence on the study design, the collection, analysis or interpretation of data, the writing of the report or the decision to submit the article for publication.

Declaration of Competing Interest

The authors declare that they have no known competing financial interests or personal relationships that could have appeared to influence the work reported in this paper.

Appendix A. Supplementary data

Supplementary data to this article can be found online at https://doi.org/10.1016/j.ctro.2023.100630.

References

[1] Ahmadi N, Chan M, Huo YR, Sritharan N, Chin RY. Survival outcome of tonsillar squamous cell carcinoma (TSCC) in the context of human papillomavirus (HPV): A systematic review and meta-analysis. Surgeon 2019;17(1):6–14.
[2] Avril D, Foy J-P, Bouaoud J, Grégoire V, Saintigny P. Biomarkers of radioresistance in head and neck squamous cell carcinomas. Int J Radiat Biol 2023;99(4):583–93.
[3] Hutchinson M-K, Mierzwa M, D'Silva NJ. Radiation resistance in head and neck squamous cell carcinoma: dire need for an appropriate sensitizer. Oncogene 2020;39(18):3638–49.
[4] Krishnamurthy S, Ahmed I, Bhise R, Mohanti BK, Sharma A, Rieckmann T, et al. The dogma of Cetuximab and Radiotherapy in head and neck cancer - A dawn to dusk journey. Clin Transl Radiat Oncol 2022;34:75–81.
[5] Hintelmann K, Kriegs M, Rothkamm K, Rieckmann T. Improving the Efficacy of Tumor Radiosensitization Through Combined Molecular Targeting. Front Oncol 2020;10:1260.
[6] Morgan MA, Parsels LA, Maybaum J, Lawrence TS. Improving the efficacy of chemoradiation with targeted agents. Cancer Discov. 2014;4:280-91.
[7] Carruthers RD, Ahmed SU, Ramachandran S, Strathdee K, Kurian KM, Hedley A, et al. Replication Stress Drives Constitutive Activation of the DNA Damage Response and Radioresistance in Glioblastoma Stem-like Cells. Cancer Res. 2018;78:5060-71.
[8] Karnak D, Engelke CG, Parsels LA, Kausar T, Wei D, Robertson JR, et al. Combined inhibition of Wee1 and PARP1/2 for radiosensitization in pancreatic cancer. Clin Cancer Res Offi J Am Assoc Cancer Res. 2014;20:5085-96.
[9] Parsels LA, Engelke CG, Parsels J, Flanagan SA, Zhang Q, Tanska D, et al. Combinatorial Efficacy of Olaparib with Radiation and ATR Inhibitor Requires PARP1 Protein in Homologous Recombination-Proficient Pancreatic Cancer. Mol Cancer Ther. 2021;20:263-73.
[10] Parsels LA, Karnak D, Parsels JD, Zhang Q, Velez-Padilla J, Reichert ZR, et al. PARP1 Trapping and DNA Replication Stress Enhance Radiosensitization with Combined WEE1 and PARP Inhibitors. Mol Cancer Res. 2018;16:222-32.
[11] Vance S, Liu E, Zhao L, Parsels JD, Parsels LA, Brown JL, et al. Selective radiosensitization of p53 mutant pancreatic cancer cells by combined inhibition of Chk1 and PARP1. Cell Cycle 2011;10(24):4321–9.
[12] Satoh MS, Lindahl T. Role of poly(ADP-ribose) formation in DNA repair. Nature 1992;356(6367):356–8.
[13] Wang M, Wu W, Wu W, Rosidi B, Zhang L, Wang H, et al. PARP-1 and Ku compete for repair of DNA double strand breaks by distinct NHEJ pathways. Nucleic Acids Res. 2006;34:6170-82.
[14] Curtin NJ. Targeting the DNA damage response for cancer therapy. Biochem Soc Trans 2023;51(1):207–21.
[15] Jannetti SA, Zeglis BM, Zalutsky MR, Reiner T. Poly(ADP-Ribose)Polymerase (PARP) Inhibitors and Radiation Therapy. Front Pharmacol 2020;11:170.
[16] Cancer Genome Atlas N. Comprehensive genomic characterization of head and neck squamous cell carcinomas. Nature. 2015;517:576-82.
[17] Hauge S, Eek Mariampillai A, Rodland GE, Bay LTE, Landsverk HB, Syljuasen RG. Expanding roles of cell cycle checkpoint inhibitors in radiation oncology. Int J Radiat Biol 2021;1–10.
[18] Chera BS, Sheth SH, Patel SA, Goldin D, Douglas KE, Green RL, et al. Phase 1 trial of adavosertib (AZD1775) in combination with concurrent radiation and cisplatin for intermediate-risk and high-risk head and neck squamous cell carcinoma. Cancer 2021;127(23):4447–54.
[19] Forster M, Mendes R, Guerrero Urbano T, Evans M, Lei M, Spanswick V, et al. ORCA-2: A phase I study of olaparib in addition to cisplatin-based concurrent chemoradiotherapy for patients with high risk locally advanced (LA) squamous cell carcinoma of the head and neck (HNSCC). Ann Oncol 2021;32(Supplement 5):789–90.
[20] Karam SD, Reddy K, Blatchford PJ, Waxweiler T, DeLouize AM, Oweida A, et al. Final Report of a Phase I Trial of Olaparib with Cetuximab and Radiation for Heavy Smoker Patients with Locally Advanced Head and Neck Cancer. Clinical Cancer Res Off J Am Assoc Cancer Res. 2018;24:4949-59.
[21] Yang ES, Deutsch E, Mehmet A, Fayette J, Tao Y, Nabell L, et al. A Phase 1b trial of prexasertib in combination with chemoradiation in patients with locally advanced head and neck squamous cell carcinoma. Radiother Oncol 2021;157:203–9.
[22] Hintelmann K, Berenz T, Kriegs M, Christiansen S, Gatzemeier F, Struve N, et al. Dual Inhibition of PARP and the Intra-S/G2 Cell Cycle Checkpoints Results in Highly Effective Radiosensitization of HPV-Positive HNSCC Cells. Front Oncol 2021;11:683688.
[23] Bußmann L, Hoffer K, Bargen CM, Droste C, Lange T, Kemmling J, et al. Analyzing tyrosine kinase activity in head and neck cancer by functional kinomics: Identification of hyperactivated Src family kinases as prognostic markers and potential targets. Int J Cancer 2021;149(5):1166–80.
[24] Zech HB, Berger J, Mansour WY, Nordquist L, von Bargen CM, Bußmann L, et al. Patient derived ex vivo tissue slice cultures demonstrate a profound DNA double-strand break repair defect in HPV-positive oropharyngeal head and neck cancer. Radiother Oncol 2022;168:138–46.
[25] Kostopoulou ON, Zupancic M, Pont M, Papin E, Lukoseviciute M, Mikelarena BA, et al. Targeted Therapy of HPV Positive and Negative Tonsillar Squamous Cell Carcinoma Cell Lines Reveals Synergy between CDK4/6, PI3K and Sometimes FGFR Inhibitors, but Rarely between PARP and WEE1 Inhibitors. Viruses 2022;14(7):1372.
[26] Kimple RJ, Smith MA, Blitzer GC, Torres AD, Martin JA, Yang RZ, et al. Enhanced radiation sensitivity in HPV-positive head and neck cancer. Cancer Res. 2013;73:4791-800.
[27] Rieckmann T, Tribius S, Grob TJ, Meyer F, Busch C-J, Petersen C, et al. HNSCC cell lines positive for HPV and p16 possess higher cellular radiosensitivity due to an impaired DSB repair capacity. Radiother Oncol 2013;107(2):242–6.
[28] Beck H, Nähse-Kumpf V, Larsen MSY, O'Hanlon KA, Patzke S, Holmberg C, et al. Cyclin-dependent kinase suppression by WEE1 kinase protects the genome through control of replication initiation and nucleotide consumption. Mol Cell Biol 2012;32(20):4226–36.
[29] Moiseeva TN, Qian C, Sugitani N, Osmanbeyoglu HU, Bakkenist CJ. WEE1 kinase inhibitor AZD1775 induces CDK1 kinase-dependent origin firing in unperturbed G1- and S-phase cells. Proc Natl Acad Sci U S A 2019;116(48):23891–3.
[30] Cuneo KC, Morgan MA, Davis MA, Parcels LA, Parcels J, Karnak D, et al. Wee1 Kinase Inhibitor AZD1775 Radiosensitizes Hepatocellular Carcinoma Regardless of TP53 Mutational Status Through Induction of Replication Stress. Int J Radiat Oncol Biol Phys 2016;95(2):782–90.
[31] Mei M, Chen YH, Meng T, Qu LH, Zhang ZY, Zhang X. Comparative efficacy and safety of radiotherapy/cetuximab versus radiotherapy/chemotherapy for locally advanced head and neck squamous cell carcinoma patients: a systematic review of published, primarily non-randomized, data. Ther Adv Med Oncol. 2020;12:1758835920975355.
[32] Bourhis J, Tao Y, Sun X, Sire C, Martin L, Liem X, et al. Avelumab-cetuximab-radiotherapy versus standards of care in patients with locally advanced squamous cell carcinoma of head and neck (LA-SCCHN): Randomized phase III GORTEC-REACH trial (Abstract LBA35). Ann Oncol 2021;32(Supplement 5):S1310.
[33] Lee NY, Ferris RL, Psyrri A, Haddad RI, Tahara M, Bourhis J, et al. Avelumab plus standard-of-care chemoradiotherapy versus chemoradiotherapy alone in patients with locally advanced squamous cell carcinoma of the head and neck: a randomised, double-blind, placebo-controlled, multicentre, phase 3 trial. Lancet Oncol 2021;22(4):450–62.
[34] Machiels J, Tao Y, Burtness B, Tahara M, Rischin D, Alves GV, et al. Primary results of the phase III KEYNOTE-412 study: Pembrolizumab (pembro) with chemoradiation therapy (CRT) vs placebo plus CRT for locally advanced (LA) head and neck squamous cell carcinoma (HNSCC) (Abstract LBA5). Ann Oncol 2022;32(Supplement 7):S808–69.
[35] Rassamegevanon T, Lock S, Baumann M, Krause M, von Neubeck C. Comparable radiation response of ex vivo and in vivo irradiated tumor samples determined by residual gammaH2AX. Radiother Oncol 2019;139:94–100.
[36] Menegakis A, De Colle C, Yaromina A, Hennenlotter J, Stenzl A, Scharpf M, et al. Residual gammaH2AX foci after ex vivo irradiation of patient samples with known tumour-type specific differences in radio-responsiveness. Radiother Oncol 2015;116:480–5.
[37] Elsesy ME, Oh-Hohenhorst SJ, Löser A, Oing C, Mutiara S, Köcher S, et al. Second-Generation Antiandrogen Therapy Radiosensitizes Prostate Cancer Regardless of Castration State through Inhibition of DNA Double Strand Break Repair. Cancers (Basel) 2020;12(9):2467.
[38] Köcher S, Beyer B, Lange T, Nordquist L, Volquardsen J, Burdak-Rothkamm S, et al. A functional ex vivo assay to detect PARP1-EJ repair and radiosensitization by PARP-inhibitor in prostate cancer. Int J Cancer 2019;144(7):1685–96.
[39] Köcher S, Zech HB, Krug L, Gatzemeier F, Christiansen S, Meyer F, et al. A Lack of Effectiveness in the ATM-Orchestrated DNA Damage Response Contributes to the DNA Repair Defect of HPV-Positive Head and Neck Cancer Cells. Front Oncol 2022;12:765968.
[40] Busch CJ, Kriegs M, Laban S, Tribius S, Knecht R, Petersen C, et al. HPV-positive HNSCC cell lines but not primary human fibroblasts are radiosensitized by the inhibition of Chk1. Radiother Oncol 2013 Sep;108(3):495–9.